

# W pair production and decay at LEP

Franco Ligabue

*Scuola Normale Superiore, Pisa*

## Abstract

Methods for the reconstruction of W pair decays at LEP II are briefly reviewed. From the analysis of about  $55 \text{ pb}^{-1}$  data collected per experiment in 1997 at a centre-of-mass energy of 183 GeV, preliminary results on W pair production are presented, including measurements of the total cross section and of W decay branching fractions. New preliminary results on determination of the W mass from direct reconstruction are also presented.



# 1 Introduction

The LEP II programme successfully started in June 1996 when the centre-of-mass energy of  $e^+e^-$  collisions was first set to 161 GeV, allowing the first on-shell  $W^+W^-$  pairs to be produced and reconstructed by the four LEP experiments. The measurement of the W pair production cross-section led to the first W mass determination at LEP [1]. In the second half of 1996 the centre-of-mass energy was raised to 172 GeV, and about  $10 \text{ pb}^{-1}$  per experiment were delivered which allowed the first results on W mass measurement from direct reconstruction [2]. In 1997 the beam energy was further raised and each experiment collected about  $55 \text{ pb}^{-1}$  at  $\sqrt{s} = 183 \text{ GeV}$

At centre-of-mass energies well above the pair-production threshold, the total cross-section measurement no longer gives significant information on the value of the mass, but it provides an important test of the Standard Model, especially concerning the existence of the triple gauge boson coupling ZWW, which was already established by the data at 172 GeV. On the other hand, the higher cross-section allows the determination of the W mass by direct reconstruction with good statistical precision. The unique LEP feature of W bosons being produced in pairs allows the simultaneous measurement of production cross section and decay branching fractions.

In the following, the methods used by the four experiments to select W pair events are briefly reviewed. In section 3 the preliminary cross-section results at  $\sqrt{s} = 183 \text{ GeV}$  are presented, together with the branching ratio determinations using data at all beam energies, with and without the assumption of lepton universality. Interesting results on the indirect determination on  $|V_{cs}|$  are also given. In section 4 the methods for the measurement of  $M_W$  from reconstructed W pair events are reviewed, and preliminary results are given for the data collected in 1997.

## 2 Event Selection

Several selection algorithms are used by the four experiments to select W pair events according to the possible W decay channels, which give rise to distinct final state topologies. The complexity of the selection algorithms and the background contamination increase with the number of hadronic jets in the final state. Events are generally divided into three categories:

**Fully leptonic** ( $W^+W^- \rightarrow \ell^+\nu\ell^-\bar{\nu}$ ) Final states where both W's decay to a lepton-neutrino pair are characterised by low charged track multiplicity, large missing energy and momentum due to the two energetic neutrinos, and by the presence of two highly acollinear and acoplanar energetic tracks (electrons or muons from the W decay, or tracks from single-prong tau decays) or collimated low multiplicity jets from tau decays.

The main background comes from  $e^+e^- \rightarrow \gamma\gamma$  and  $e^+e^- \rightarrow Z\gamma$  events, but it's highly reduced by topological cuts such as the request of high transverse missing momentum with respect to the beam axis. The fraction of fully leptonic final states is expected to be 10.4% from the Standard Model.

Selection algorithms based on event topology are combined with lepton identification algorithm and the selected events are classified according to the candidate lepton flavour. Lepton misidentification especially in the case of  $\tau \rightarrow e$ ,  $\tau \rightarrow \mu$  decays leads to migration between the various lepton flavour channels, expressed in terms of non-zero diagonal terms in the  $9 \times 9$  efficiency matrix, determined from Monte Carlo. The global efficiency for the fully leptonic selection ranges from 56% to 77%. Purities are typically very high, ranging from 90% to 95%

**Semileptonic** ( $W^+W^- \rightarrow q\bar{q}\ell\nu$ ) Final states where only one of the W's decays leptonically are expected to represent 43.7% of  $W^+W^-$  decays in the Standard Model. They are selected based on the presence of a high energy neutrino, showing as large missing momentum pointing at a large angle with respect to the beam direction, and of a high-energy lepton usually isolated from the two hadronic jets. The main backgrounds come from radiative Z returns  $e^+e^- \rightarrow q\bar{q}\gamma$  events and from four-fermion  $e^+e^- \rightarrow q\bar{q}\ell\bar{\ell}$  events.

Selection algorithms involve the use of many variables, which are sometimes combined to give a “likelihood” for an event to be signal, evaluated from Monte Carlo simulation.

Efficiencies are again expressed in terms of a  $3 \times 3$  matrix with non-zero off-diagonal terms accounting for channel migration due to lepton misidentification. The overall signal efficiency for the semileptonic selection ranges from 73% to 88%, with typical purities from 90% to 96% .

**Fully Hadronic** ( $W^+W^- \rightarrow q\bar{q}q\bar{q}$ ) This channel accounts for 45.9% of W pair decays according to the Standard Model. Fully hadronic final states are characterised by no missing energy and momentum, and a four-jet topological structure with high sphericity, and high track multiplicity. Due to the comparatively huge  $e^+e^- \rightarrow q\bar{q}(\gamma)$  cross-section, tails in the multijet production distributions from hard gluon emission cause a sizeable

amount of background to be effectively irreducible, and make it hard to devise a simple discriminating technique.

Therefore, all four experiments make use of multivariable discrimination algorithms — *e.g.* neural networks [3], [5] — which combine the information from many event variables, each containing some signal-background separation power, which is however not large enough for a simple combination of variables to be effective.

Efficiencies for typical cuts on the discriminating variable range approximately from 78% to 88%, while purities, which are limited by the irreducible QCD background, are around 80% .

### 3 Cross-section and Branching Fractions

The number of events selected in the various decay channels are used to extract the  $W^+W^-$  production cross section and the  $W$  decay branching fractions.

Efficiency matrices and background contamination are estimated from Monte Carlo simulation, except for the fully hadronic channel, where the number of selected signal events can alternatively be extracted from a fit to the neural network output distribution [3],[5] the signal and background shapes being taken from Monte Carlo. The small contribution from non-CC03 diagrams is corrected for, either by direct subtraction of the expected number of events or by means of a multiplicative factor, both estimated from Monte Carlo.

The number of signal events in each channel can be expressed in terms of the total  $W^+W^-$  cross section and of the  $W$  branching fractions. Several fits can be performed:

- the three leptonic branching fractions can be fitted independently assuming

$$B(W \rightarrow e\nu) + B(W \rightarrow \mu\nu) + B(W \rightarrow \tau\nu) + B(W \rightarrow q\bar{q}) = 1$$

The results from the four experiments, from data at all centre-of-mass energies, are listed in table 1: they are consistent with lepton universality and with the Standard model prediction of 10.8%

- lepton universality can be assumed and  $B(W \rightarrow q\bar{q})$  can be fitted, again assuming that leptonic and hadronic branching fractions add up to unity. The results are listed in table 2

	$B(W \rightarrow e\nu)$ (%)	$B(W \rightarrow \mu\nu)$ (%)	$B(W \rightarrow \tau\nu)$ (%)
ALEPH	$11.2 \pm 0.8 \pm 0.3$	$9.9 \pm 0.8 \pm 0.2$	$9.7 \pm 1.0 \pm 0.3$
DELPHI	$9.9 \pm 1.1 \pm 0.5$	$11.4 \pm 1.1 \pm 0.5$	$11.2 \pm 1.7 \pm 0.7$
L3	$10.7 \pm 0.9 \pm 0.2$	$10.3 \pm 0.9 \pm 0.2$	$9.2 \pm 1.2 \pm 0.3$
OPAL	$11.7 \pm 0.9 \pm 0.3$	$10.1 \pm 0.8 \pm 0.3$	$10.3 \pm 1.0 \pm 0.3$
Combined	$11.0 \pm 0.5$	$10.3 \pm 0.5$	$10.0 \pm 0.6$

Table 1: Summary of W leptonic branching fractions measurements at LEP II, using data at all centre-of-mass energies

	$B(W \rightarrow \text{had})$ (%)
ALEPH	$69.0 \pm 1.2 \pm 0.6$
DELPHI	$67.5 \pm 1.5 \pm 0.9$
L3	$69.5 \pm 1.3 \pm 0.4$
OPAL	$67.9 \pm 1.2 \pm 0.6$
Combined	$68.6 \pm 0.8$

Table 2: Summary of W hadronic branching fraction measurements at LEP II, using data at all centre-of-mass energies. Lepton universality is assumed

	$\sigma_{CC03}$ (pb)
ALEPH	$15.51 \pm 0.61 \pm 0.36$
DELPHI	$16.01 \pm 0.71 \pm 0.43$
L3	$16.66 \pm 0.66 \pm 0.30$
OPAL	$15.52 \pm 0.62 \pm 0.35$
Combined	$15.90 \pm 0.41$

Table 3: Summary of WW pair production cross section measurements, at  $\sqrt{s} = 183$  GeV. In the combined total error, 0.20 pb are from common systematics

- assuming Standard Model values for the decay branching ratios, the total production cross section  $\sigma_{CC03}$  can be fitted. The results, listed in table 3 are well consistent with the values obtained when the Standard Model constraints on the branching fractions are released

The preliminary result for the combined cross section is

$$\sigma_{CC03} = (15.90 \pm 0.41) \text{ pb}$$

at a luminosity-weighted average centre-of-mass energy of  $182.68 \pm 0.06 \text{ GeV}$

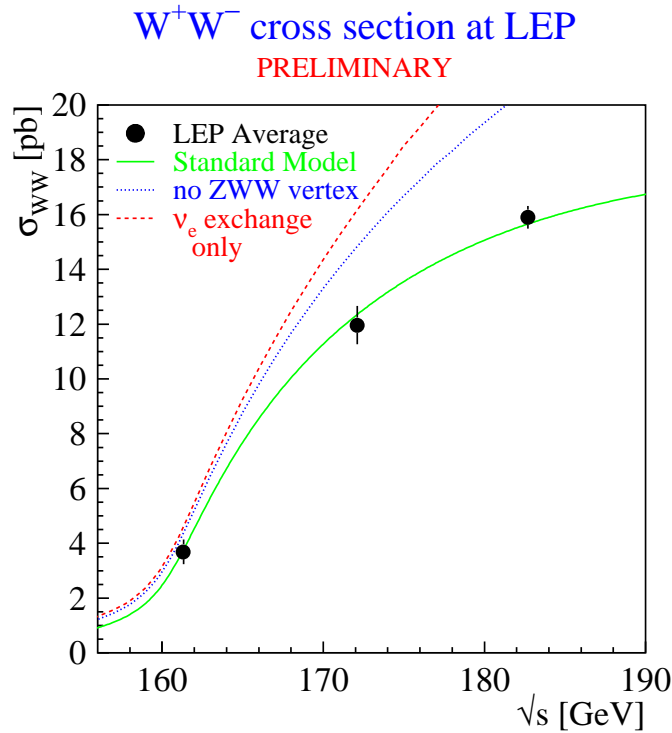


Figure 1: Measured total WW production cross-section as a function of centre-of-mass energy .

Figure 1 compares the values of  $\sigma_{CC03}$  measured by LEP as a function of  $\sqrt{s}$  to the Standard Model prediction: models excluding the existence of the trilinear gauge boson couplings are strongly disfavoured by the LEP data

	$ V_{cs} $
ALEPH [7]	$1.00 \pm 0.10 \pm 0.06$
DELPHI[8]	$0.87^{+0.26}_{-0.22} \pm 0.11$
L3[9]	$0.98 \pm 0.22 \pm 0.08$

Table 4: Recent determinations of  $|V_{cs}|$  from direct charm counting in  $W$  decays at LEP II

### 3.1 Determination of $|V_{cs}|$

In the Standard Model, the  $W$  decay branching ratio into hadrons can be expressed in terms of the relevant Cabibbo-Kobayashi-Maskawa matrix elements:

$$\frac{B(W \rightarrow \text{had})}{1 - B(W \rightarrow \text{had})} = \left(1 + \frac{\alpha_s}{\pi}\right) \sum_{i=u,c; j=d,s,b} |V_{ij}|^2$$

The precise measurement of  $B(W \rightarrow \text{had})$  can be used to derive a constraint on  $|V_{cs}|$  assuming the present world average values for the other matrix elements, and using [18]  $\alpha_s(M_z) = 0.118 \pm 0.003$

The result is

$$|V_{cs}| = 1.03 \pm 0.04$$

where the error is dominated by the statistical uncertainty on the  $W$  hadronic branching ratio.

An alternative indirect measurement of  $|V_{cs}|$  comes from the direct measurement of the charm fraction in  $W$  hadronic decays.

$$f_c \equiv \frac{\Gamma(W \rightarrow \text{cs})}{\Gamma(W \rightarrow \text{had})} = \frac{|V_{cd}|^2 + |V_{cs}|^2 + |V_{cb}|^2}{|V_{ud}|^2 + |V_{us}|^2 + |V_{ub}|^2 + |V_{cd}|^2 + |V_{cs}|^2 + |V_{cb}|^2}$$

Charm-tagging [7],[9] and jet-flavour tagging [8] algorithms have been developed, which allow the separation of charm events among the decays of the  $W$  and hence the determination of  $f_c$  at LEP II.

The results are shown in table 4.

## 3.2 Invisible Width

The total cross section measurement can be interpreted as a measurement of possible deviations from the Standard Model prediction, in the particular scenario [10] where such deviations are in the form of effectively invisible decays of the W (*i.e.* decays where the single charged decay product would be so soft as to remain undetected). One of the effects of such invisible decays of the W would be that of reducing the visible cross-section by reducing  $B(W \rightarrow \text{visible})$ . Another effect would be the presence of events where only one of the pair-produced W bosons decays invisibly. These events can be directly searched for within the search for single W production [11].

An analysis [3] based on the ALEPH cross-section measurements as a function of  $\sqrt{s}$  gives

$$\Gamma_W^{\text{invis}} = (35_{-48}^{+52} \pm 37) \text{ MeV}$$

which, if interpreted as a measurement of the total W width, gives:

$$\Gamma_W = (2.135_{-0.048}^{+0.052} \pm 0.037) \text{ GeV}$$

## 4 Mass measurement from direct reconstruction

Only the fully hadronic and semileptonic decay channels are used for the determination of the W mass from direct reconstruction.

### 4.1 Kinematic fit

Since the energy of hadronic jets is measured with relatively poor precision, all experiments perform a kinematic fitting procedure to recompute the jet momenta, imposing energy and momentum conservation, and allowing the energy and direction of each jet to vary within the expected resolution around the expected central value. In semileptonic events, the neutrino energy and direction are determined from momentum conservation. In principle each event provides two invariant masses, one for each decaying W. In most cases however, the average invariant mass is computed by adding the additional constraint of equal masses in the fit: this is always done for the semileptonic channel, while for the hadronic case some experiments [15],[16] decided to exploit the information from both invariant masses.



## 4.2 Jet pairing

In the fully hadronic channel, only one out of three possible di-jet combinations (ten in the case of five jets in the final state) is the correct one. Various techniques are employed to define the best combination, using for instance the difference between the two invariant masses from the kinematic fit, or the fit  $\chi^2$ . Since these methods are never perfectly efficient, all experiment recover some information from second best combinations. DELPHI [16] for instance, combines the information from all possible jet pairings, after computing a probability for each combination to be the correct one, based on candidate W production angles.

## 4.3 Determination of $M_W$

The event-by-event invariant mass from the kinematic fit provides an estimator for  $M_W$  from which the value of the W mass has to be extracted. Figure 2 shows some of the invariant mass distributions obtained by the experiments.

The extracton of  $M_W$  can be achieved basically in two ways:

- by parametrizing the invariant mass distribution (which can be two-dimensional, in case two masses per event are considered) with a functional shape containing  $M_W$  as a parameter. Usually a Breit-Wigner shape is used, possibly convoluted with phase-space and resolution functions.
- by comparing the invariant mass distribution obtained from data to the same distribution from simulation for different input  $M_W$  values, and determining the best value for  $M_W$  from a maximum-likelihood fit. Since sufficiently large samples of Monte Carlo events can only be generated for few input mass values, a reweighting technique is employed to obtain a Monte Carlo distribution for any new value of  $M_W$ : each event is assigned a weight which accounts for the changed differential production cross-section.

The first method does not provide an unbiased value for  $M_W$ , essentially because of distorsions due to initial state radiation and to detector effects. It has the advantage, however, of allowing the use of an event-by-event mass error [16]. It is found from simulation that a simple linear relation holds between the generated and the fitted mass (calibration curve) which is used to correct the fit result.

The second method is intrinsically unbiased and automatically takes into account initial state radiation and detector effects, provided they are correctly simulated by the Monte Carlo.

Generally, both methods are used in order to provide a cross check of the mass measurement, though only one is chosen for the quoted result.

Checks are made on the reliability of the statistical error given from the mass fit, by generating a large number of Monte Carlo samples of the same size of the data sample, and by looking at the fit error and pull distributions.

## 4.4 Systematics

The most relevant sources of systematic errors which are not correlated among the four experiments include finite Monte Carlo statistics and detector effects. The latter basically enter at the kinematic fitting level, as uncertainties on the expected jet momenta and resolutions.

Correlated systematics include uncertainties on the simulation of initial state radiation and of hadronization processes, as well as on the simulation of non-CC03 four-fermion processes.

**Beam Energy** An important role is played by the error on the LEP beam energy: although W pair decays are directly reconstructed, the energy conservation constraint imposed by the kinematic fitting procedure introduces an effective linear dependence on the fitted mass value:

$$\frac{\Delta M_W}{M_W} = \frac{\Delta E_{\text{LEP}}}{E_{\text{LEP}}}$$

A value  $\Delta E_{\text{LEP}} = 30 \text{ MeV}$  is used for the preliminary results at  $\sqrt{s} = 183 \text{ GeV}$

**Final State Interaction** The other dominant source of correlated systematics is the possibility of Final State Interactions (FSI) in the fully hadronic channel: Bose-Einstein correlation between same-charge pions, and cross-talk at hadronization level between the two hadronically decaying W's (Colour Reconnection), can in principle affect the value of  $M_W$  mass when measured in the fully hadronic channel. While Bose-Einstein effects have been measured at LEP I [13], at present there is no evidence within experimental errors of Colour Reconnection effects at LEP II, which would show for instance in a difference

	$\ell\nu q\bar{q}$ $M_W$ (GeV/ $c^2$ )	$q\bar{q}q\bar{q}$ $M_W$ (GeV/ $c^2$ )	combined $M_W$ (GeV/ $c^2$ )
ALEPH	$80.16 \pm 0.20 \pm 0.08$	$80.45 \pm 0.18 \pm 0.12$	$80.30 \pm 0.13 \pm 0.09$
DELPHI	$80.50 \pm 0.26 \pm 0.07$	$80.02 \pm 0.20 \pm 0.11$	$80.30 \pm 0.16 \pm 0.08$
L3	$80.03 \pm 0.24 \pm 0.07$	$80.51 \pm 0.21 \pm 0.13$	$80.32 \pm 0.16 \pm 0.09$
OPAL	$80.25 \pm 0.18 \pm 0.08$	$80.48 \pm 0.23 \pm 0.13$	$80.34 \pm 0.14 \pm 0.08$

Table 5: Summary of  $M_W$  determinations at LEP II. Separate results for the hadronic and semileptonic channels are shown, as well as their combination. For all results, the first error is statistical, the second is systematic. See ref. [17] for a more detailed error breakdown

in the charged-particle multiplicity distribution between fully hadronic and semi-leptonic decays [6].

A systematic uncertainty of 100 MeV has been assigned by all experiments to the mass measurement in the hadronic channel: this value is either taken from previous estimates [14] or from studies [12] on Monte Carlo samples where Bose-Einstein and Colour Reconnection effects were alternatively implemented and switched off.

## 4.5 Results for $M_W$

The results for the four LEP experiments at  $\sqrt{s} = 183$  GeV are summarized in table 5.

The combined [17] preliminary results for the semileptonic and hadronic channels are

$$M_W^{\ell\nu q\bar{q}} = (80.22 \pm 0.11_{\text{exp}} \pm 0.03_{\text{LEP}}) \text{ GeV}/c^2$$

$$M_W^{q\bar{q}q\bar{q}} = (80.36 \pm 0.08_{\text{exp}} \pm 0.10_{\text{FSI}} \pm 0.03_{\text{LEP}}) \text{ GeV}/c^2$$

where the first error includes statistical and systematic contributions. The systematic errors from Final State Interaction and from beam energy uncertainty have been singled out. The combined value is

$$M_W = (80.30 \pm 0.08_{\text{exp}} \pm 0.05_{\text{FSI}} \pm 0.03_{\text{LEP}}) \text{ GeV}/c^2$$

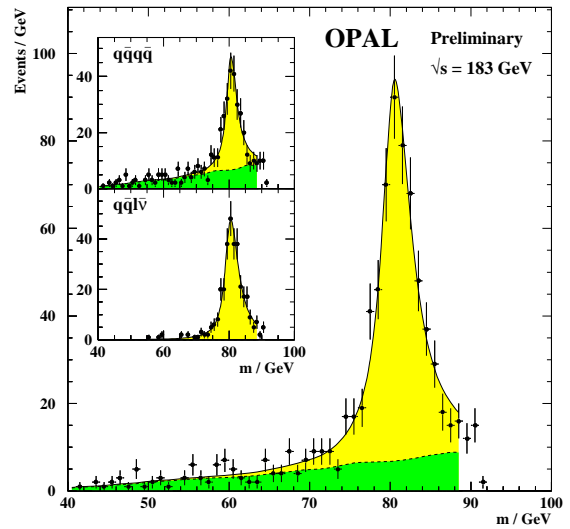
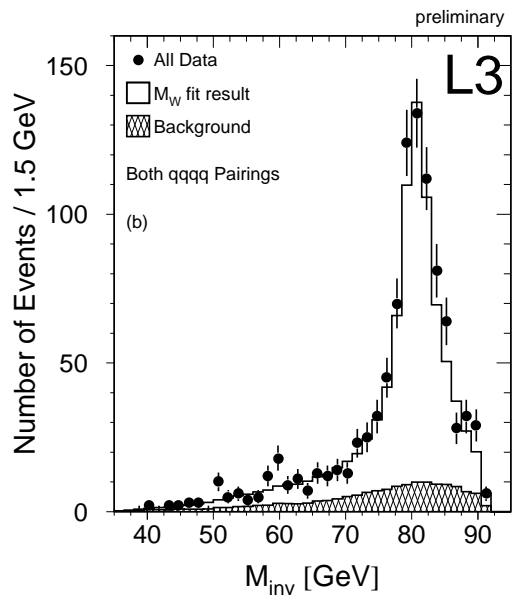
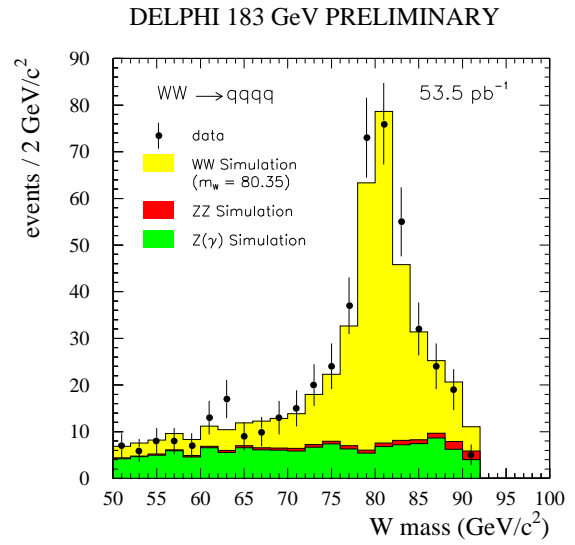
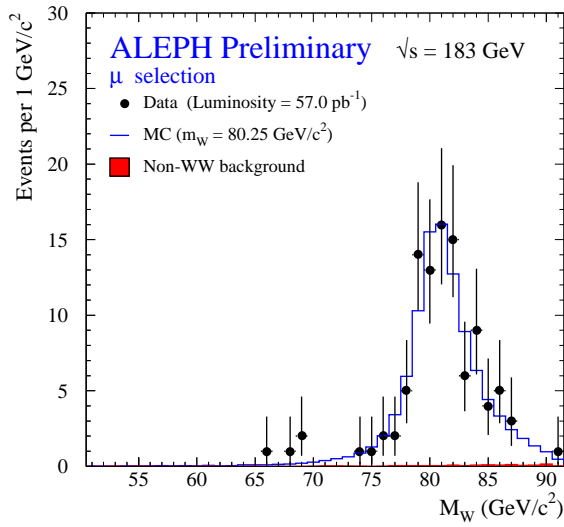


Figure 2: Examples of Invariant mass distributions from kinematic fit

	$\Gamma_W$ ( GeV/ $c^2$ )
L3	$2.41 \pm 0.39 \pm 0.25$
OPAL	$2.25^{+0.39}_{-0.35} \pm 0.17$

Table 6: Results of W width determinations from simultaneous  $M_W, \Gamma_W$  fits at  $\sqrt{s} = 183$  GeV

**Combination with previous results** Combining the above results with earlier  $M_W$  measurements from direct reconstruction at  $\sqrt{s} = 172$  GeV [2] yields

$$M_W^{\ell\nu q\bar{q}} = (80.27 \pm 0.10_{\text{exp}} \pm 0.03_{\text{LEP}}) \text{ GeV}/c^2$$

$$M_W^{q\bar{q}q\bar{q}} = (80.40 \pm 0.10_{\text{exp}} \pm 0.10_{\text{FSI}} \pm 0.03_{\text{LEP}}) \text{ GeV}/c^2$$

No significant difference between the mass measurement in the hadronic channel with respect to the semileptonic one can be seen at the present level of accuracy. The combined LEP value for  $M_W$  from direct reconstruction is therefore

$$M_W = (80.34 \pm 0.07_{\text{exp}} \pm 0.05_{\text{FSI}} \pm 0.03_{\text{LEP}}) \text{ GeV}/c^2$$

Combining this result with the mass determination from pair-production cross section measurements [1] yields

$$M_W = (80.40 \pm 0.09) \text{ GeV}/c^2$$

## 4.6 Width determination

Some experiments [6],[5] perform a simultaneous fit for  $M_W$  and  $\Gamma_W$  to the invariant mass distribution, leaving both parameters free instead of assuming the Standard Model relation between the W boson mass and its width. The correlation between the two parameters turns out to be small. The results at  $\sqrt{s} = 183$  GeV, shown in table 6, are compatible with the Standard Model expectation ( $2.08 \text{ GeV}/c^2$ ) and with the current world average value from measurements at the  $p\bar{p}$  colliders [18], although they are not competitive due to the large errors.

## 5 Conclusion

Detection and reconstruction of W bosons at LEP II has allowed the measurement of the pair-production cross section and of the W decay branching fraction, which provide an important test of the Standard Model, as well as an increasingly precise determination of the W boson mass.

The LEP II goal of a final error on  $M_W$  of 50 MeV/ $c^2$  is not out of sight: with the 150 pb $^{-1}$  per experiment foreseen in the 1998 run, the statistical error on  $M_W$  will be of the order of 40 MeV/ $c^2$  which is smaller than the current total systematic error. Efforts must therefore be spent in order to reduce the largest systematic contributions, especially the LEP energy error and the Final State Interaction uncertainty.

## References

- [1] ALEPH Collaboration, Phys. Lett. **B 401** (1997) 347 ;  
DELPHI Collaboration, P. Abreu *et al.*, Phys. Lett. **B 397** (1997) 158 ;  
L3 Collaboration, M. Acciarri *et al.*, Phys. Lett. **B 398** (1997) 223 ;  
OPAL Collaboration, K. Ackerstaff *et al.* Phys. Lett. **B 389** (1996) 416
- [2] ALEPH Collaboration, CERN-PPE/97-164 ;  
DELPHI Collaboration, P. Abreu *et al.*, CERN-PPE/97-160 accepted by European Physical Journal C ;  
L3 Collaboration, M. Acciarri *et al.*, Phys. Lett. **B 407** (1997) 419 ;  
OPAL Collaboration, K. Ackerstaff *et al.*, CERN-PPE/97-116 European Physical Journal **C1** (1998) 395
- [3] ALEPH Collaboration, ALEPH note 98-019 CONF-98-009
- [4] DELPHI Collaboration, DELPHI note 98-20 CONF 120
- [5] L3 Collaboration, L3 note 2236
- [6] OPAL Collaboration, OPAL Physics Note PN331 (internal note)
- [7] ALEPH Collaboration, ALEPH note 98-011 CONF-98-001
- [8] DELPHI Collaboration, DELPHI note 97-114 CONF 96

- [9] L3 Collaboration, L3 note 2232
- [10] J. Kalinowski and P.M. Zerwas, Phys. Lett. **B 400** (1997) 112
- [11] ALEPH Collaboration, ALEPH/98-023, CONF/98-013
- [12] ALEPH Collaboration, CERN-PPE/97-164 ;
- [13] ALEPH Collaboration, *Bose-Einstein correlations in W-pair decays*, Contribution to the EPS '97 Conference in Jerusalem (ref. 590)
- [14] Proceedings of CERN LEP2 Workshop, CERN 96-01, Vol.1, eds. G.Altarelli *et al.*, 1996
- [15] ALEPH Collaboration, ALEPH note 98-020 CONF-98-010
- [16] DELPHI Collaboration, DELPHI note 98-27 CONF 123
- [17] LEP Electroweak Working Group, note LEPEWWG/MW/98-01
- [18] R.M. Barnett *et al.*, *Review of Particle Properties* Phys. Rev. **D 54** (1996)